Articles in PresS. J Neurophysiol (August 25, 2010). doi:10.1152/jn.00253.2010

Multiple somatotopic representations of heat and mechanical pain in the operculo-insular cortex: a high-resolution fMRI study

Ulf Baumgärtner[a,*], Gian Domenico Iannetti[b,c,*], Laura Zambreanu[c,d]
Peter Stoeter[e], Rolf-Detlef Treede[a], and Irene Tracey[d]

a: Department of Neurophysiology, Center for Biomedicine and Medical Technology (CBTM), Medical Faculty Mannheim, Heidelberg University, Mannheim, Germany
b: Department of Neuroscience, Physiology and Pharmacology, University College London, London, UK
c: Department of Physiology, Anatomy and Genetics, University of Oxford, Oxford, UK
d: Oxford Centre for Functional Magnetic Resonance Imaging of the Brain (FMRIB), Clinical Neurology and Nuffield Department Anaesthetics, University of Oxford, Oxford, UK
e: Department of Neuroradiology, Johannes Gutenberg University, Mainz, Germany

* These authors contributed equally

Running title: Multiple pain representations in the operculoinsular cortex

Address for correspondence

Dr. med. Ulf Baumgärtner
Department of Neurophysiology, Center for Biomedicine and Medical Technology (CBTM), Medical Faculty Mannheim, Heidelberg University, Ludolf-Krehl-Str. 13-17, 68167 Mannheim, Germany
phone: +49-621-383-9934, Fax: +49-621-383-99321
e-mail: ulf.baumgaertner@medma.uni-heidelberg.de

Key words: somatotopy; pain; noxious heat; imaging; laser stimulation; pin prick stimulation.

Abbreviations

ANOVA	analysis of variance
BOLD effect	blood oxygen level dependent (effect); correlate of cerebral activation
fMRI	functional magnetic resonance imaging
FSL	FMRIB's Software Library
MNI	Montreal Neurological Institute
ROI	region of interest
SI	primary somatosensory cortex
SII / PV	secondary somatosensory cortex / parietal ventral area

Summary

Whereas studies of somatotopic representation of touch have been useful to distinguish multiple somatosensory areas within SI and SII regions, no such analysis exists for the representation of pain across nociceptive modalities. Here, we investigated somatotopy in the operculo-insular cortex with noxious heat and pin prick stimuli in eleven healthy subjects using high-resolution (2x2x4 mm) 3T fMRI. Heat stimuli (delivered using a laser) and pin prick stimuli (delivered using a punctate probe) were directed to the dorsum of the right hand and foot in a balanced design. Locations of the peak fMRI responses were compared between stimulation sites (hand vs foot) and modalities (heat vs pin prick) within four bilateral regions of interest: anterior and posterior insula, frontal and parietal operculum. Importantly, all analyses were performed on individual, non-normalised fMRI images. For heat stimuli, we found hand-foot somatotopy in the contralateral anterior and posterior insula (hand 9 mm ± 10 mm anterior to foot, mean ± SD, $p<0.05$) and in the contralateral parietal operculum (SII; hand 7 mm ± 10 mm lateral to foot, $p<0.05$). For pin prick stimuli we also found somatotopy in the contralateral posterior insula (hand 9 mm ± 10 mm anterior to foot, $p<0.05$). Furthermore, the response to heat stimulation of the hand was 11 mm ± 12 mm anterior to the response to pin prick stimulation of the hand in the contralateral (left) anterior insula ($p<0.05$). These results indicate the existence of multiple somatotopic representations for pain within the operculo-insular region in humans, possibly reflecting its importance as a sensory-integration site that directs emotional responses and behaviour appropriately depending upon the body site being injured.

Introduction

The cortical representation of innocuous somatosensory stimuli has been the subject of investigations for many decades. Detailed electrophysiological studies of receptive field somatotopies revealed multiple representations of the body within the primary (SI) and secondary (SII) somatosensory cortex in monkeys (Kaas 1983, Krubitzer et al. 1995, Fitzgerald et al. 2004), and these somatosensory subdivisions exhibited different functional properties. Functional imaging studies with tactile stimuli in humans have supported these subdivisions within SI and SII (Gelnar et al. 1998, Disbrow et al. 2000, Eickhoff et al. 2006a&b, Young et al. 2004).

The cerebral representation and processing of nociceptive stimuli has been studied quite extensively with the evolution of neuroimaging techniques. An expansive set of regions, including S1, thalamus and distinct divisions of the insular, prefrontal and anterior cingulate cortices amongst other, has been described as relevant (for review see Apkarian et al. 2005, Tracey & Mantyh 2007). Surprisingly few studies have investigated the somatotopy for nociceptive stimuli, probably because it was anticipated to be identical to that for touch. The somatotopic maps for pain and touch are similar in the thalamus, where the face is represented medially and the foot laterally (Lenz et al. 1988, 1994, 1997), and in SI, where the face is represented laterally and the foot medially (Tarkka and Treede 1993, Andersson et al. 1997, DaSilva et al. 2002, Bingel et al. 2004).

For cortical processing of painful stimuli, the operculo-insular cortex plays an important role (Treede et al. 2000). Nociceptive areas within this region include several parts of the insula deep inside the lateral sulcus, and those parts of the frontal and parietal lobes that cover the insula (called the opercula). This region receives nociceptive input as early as or even earlier

98 than SI (Tarkka and Treede 1993, Ploner et al. 1999, Rios et al. 1999, Frot and Mauguière
99 2003). Its electrical stimulation elicits painful sensations (Ostrowsky et al. 2002, Afif et al.
100 2008, Mazzola et al. 2009), whereas lesions impair pain sensitivity (Greenspan et al. 1999).
101 Furthermore, its activity is enhanced during nociceptive discrimination tasks (Schlereth et al.
102 2003), correlates reliably with perceived pain intensity (Iannetti et al. 2005), and opiate
103 receptor density is comparable to that in the cingulate cortex (Baumgärtner et al. 2006a).
104
105 For the somatotopy in the operculo-insular cortex there are two conflicting concepts: all
106 tactile representations in the parietal operculum (including SII and parietal ventral area PV)
107 are oriented similar to SI, i.e. the face laterally and the foot medially (Fitzgerald et al. 2004).
108 In contrast, nociceptive input to the dorsal insula has been suggested to derive from the
109 posterior part of the proposed ventral medial thalamic nucleus (VMpo; Craig et al 1994,
110 Craig and Dostrovsky 1997) with a completely different somatotopy: face anterior and foot
111 posterior (Craig 1995). Some studies with painful stimuli confirmed the anterior-posterior
112 somatotopy (Vogel et al. 2003, Brooks et al. 2005, Baumgärtner et al. 2006b, Henderson
113 2007), whereas others showed a medio-lateral somatotopy (Bingel et al. 2004). As a
114 combination of these two concepts, a parallel projection of spinal cord neurons to both the
115 insula and the operculum (SII) has been demonstrated very recently by a viral tracing study in
116 monkey (Dum et al. 2009).
117
118 A better understanding of the somatotopic represention of painful stimuli in the operculo-
119 insular cortex may resolve conflicting concepts of its organization. Therefore we addressed
120 these two questions: (i) whether multiple somatotopical maps exist in the operculo-insular
121 area, and (ii) whether different types of cutaneous pain (heat and pin prick) share similar
122 cortical representations.

Materials and Methods

Twelve subjects (8 males and 4 females; mean age 28 years, range 26-34 years) participated in the study after giving fully informed consent, which conformed to the guidelines of the Declaration of Helsinki (1996) and had been approved by the local ethics committee.

Laser stimulation

Infrared laser pulses selectively activate heat-sensitive Aδ- and C-nociceptors in the skin (Treede et al. 1995). They evoke a very brief pin prick-like and/or burning sensation and the input transmitted via type II A-fiber mechano-heat nociceptors (type II AMH) rapidly activates the operculo-insular cortex (Tarkka and Treede 1993, Xu et al. 1997, Iannetti et al. 2004). In the present study, nociceptive heat stimuli were generated by an infrared neodymium yttrium aluminium perovskite (Nd:YAP) laser (El.En., Florence, Italy, www.elengroup.com) with a wavelength of 1.34 µm. The laser beam was transmitted via optic fiber into the scanner room and directed to the skin area that was to be stimulated (hand or foot dorsum). The diameter of the laser beam was set at 6 mm (irradiated area ~ 28 mm^2) by focusing lenses. Laser pulses produced by Nd:YAP stimulators do not induce damage to the irradiated skin that is sometimes produced by the widely-used, high-intensity CO2-laser pulses (Cruccu et al., 2003; lannetti et al., 2003).

Pin prick stimulation

Painful mechanical stimuli were applied using a hand-held 256 mN pin prick probe that has a flat cylindrical tip (diameter 250 µm), and evokes a pin-prick sensation primarily mediated by activation of a different type of Aδ-nociceptors (type I AMH, Slugg et al. 2000, Magerl et al. 2001). These mechanical stimulators have been proven to be an adequate tool to induce pin prick pain in psychophysical and clinical investigations (Greenspan and McGillis 1994,

148 Greenspan et al. 1997, Ziegler et al. 1999, Baumgärtner et al. 2002) and are commonly used
149 as part of the protocol for quantitative sensory testing in the German Research Network on
150 Neuropathic Pain (Rolke et al., 2006).
151
152 ***Experimental paradigm***
153 Each experiment consisted of 4 different stimulation conditions: laser stimulation of the right
154 hand, laser stimulation of the right foot, pin prick stimulation of the right hand, and pin prick
155 stimulation of the right foot. In a psychophysical session prior to the fMRI experiment, the
156 intensity of both laser and pin prick stimuli was adjusted in order to achieve a similarly
157 perceived intensity of both heat and mechanically induced pain at both stimulated sites (hand,
158 foot): For the hand, we used a 256-mN pin prick probe and 1.5-J laser pulses; for the foot, we
159 used the same 256-mN pin prick probe and 2-J laser pulses. During this psychophysical
160 session, subjects were asked to rate verbally the intensity of the perceived pricking pain on a
161 numerical rating scale ranging from 0 to 10 (0= no pricking pain, 10 worst pricking pain
162 imaginable).
163
164 During the fMRI recording, stimuli were delivered in blocks of 10 repeats. Within each
165 block, stimuli of the same modality were delivered to the same body region every 11.5 s, with
166 a break of 23 s separating the last stimulus of one block from the first stimulus of the next
167 block. Each of the 4 stimulation conditions was repeated four times (16 blocks) resulting in
168 40 stimuli of the same modality (laser or pin prick) to the same body region (hand or foot); in
169 total, 160 stimuli were delivered to each subject. The order of the blocks was balanced across
170 subjects. As an example, a whole stimulation sequence for one subject is shown in Fig. 1.
171 Subjects were instructed to focus their attention on the stimuli, without any specific
172 discrimination task, and to give an average intensity rating of each block of stimuli using

173 their fingers 12.5 s after the last stimulus of that block, when the experimenter inside the
174 scanner lightly touched their left ankle. To avoid nociceptor fatigue or sensitization, the laser
175 beam or the pin prick stimulator was slightly moved after each stimulus.
176
177 ***MR Image Acquisition***
178 Functional MRI scanning was performed continuously on a 3 Tesla Varian INOVA MRI
179 system. A head-only gradient coil (Magnex SGRAD MKIII) was used with a birdcage
180 radiofrequency head coil for pulse transmission and signal reception. A high resolution,
181 gradient-echo, echo-planar imaging sequence was used for functional scans (TE =45 ms, 12
182 contiguous 4-mm axial slices, flip angle 87^0, in-plane field of view 256 x 256 mm, image
183 matrix 128 x 128) with a repetition time (TR) of 3 s over 680 volumes, corresponding to a
184 total scan time of 34 min. By examining sagittal and coronal scout images, the 12 axial slices
185 were adjusted to cover the maximum superior-inferior extent of the insula (Özcan et al.
186 2005). Furthermore, at the end of the functional scan, for each subject a T1-weighted, high-
187 resolution structural image (70 contiguous 3-mm axial slices, in-plane field of view 256 x
188 192 mm, matrix 256 x 192) was collected for verification of anatomical structures.
189
190 ***Region of interest (ROI) analysis***
191 As our intention was to analyse the somatotopy for the two types of nociceptive stimuli
192 focussing on a confined area with high spatial resolution rather than the whole brain, we
193 anatomically defined four ROIs within the operculo-insular cortex in each hemisphere (8
194 ROIs in total). Following the approach described by Bense et al (2001) and Afif et al. (2009),
195 the insular cortex was divided into an anterior part, containing the 3 short (anterior) gyri, and
196 a posterior part, containing the two long (posterior) gyri. Similarly, the opercular cortex was
197 divided into a frontal and a parietal part, using the central sulcus as the separating structure.

As the quality of the EPI scans was high enough to recognize necessary anatomical landmarks, such as the boundaries of the insular cortex and insular sulci, the sylvian fissure and the central sulcus, this ROI definition was performed on the functional, BOLD-sensitive images of each subject.

In order to obtain a measure of the structural brain variability of the subjects and to have anatomical landmarks to relate the activations to, we measured five landmarks in each hemisphere (Fig. 2) using the BOLD-sensitive images: the anterior and posterior poles of the insula (on the transversal slice where the insula appeared longest), the center of the curvature of the insula, the sulcus between the 3rd and fourth insular sulcus (anatomical separation of anterior and posterior insula) and the location where the central sulcus ends (separation frontal vs. parietal operculum). Locations of landmarks and of BOLD signal increases were measured relative to the anterior commissure (AC). Thus, the origin of axes in our data is identical to that in the brain atlases of the Montreal Neurologial Institute and Talairach.

Data Analysis

Image analysis to reveal significant brain activity based on changes in BOLD signal was performed using FEAT (part of FSL, www.fmrib.ox.ac.uk/fsl). Prior to statistical analysis, the following pre-processing steps were applied to each subject's time series of fMRI volumes: motion correction (FLIRT; Jenkinson et al., 2002), spatial smoothing using a Gaussian kernel of full width at half maximum of 2 mm, subtraction of the mean of each voxel time course from that time course, and nonlinear high-pass temporal filtering (Gaussian-weighted least-squares straight line fitting, with a high-pass filter cut-off of 50 s). The fMRI signal was then linearly modeled (Worsley and Friston, 1995) on a voxel-by- voxel

basis using a general linear model approach, with local autocorrelation correction (Woolrich et al., 2001).

Group analysis

Before the analysis of single subject data, a group analysis was carried out using a mixed-effect approach, thus generating group-representative statistical maps of brain responses to laser and pinprick stimulation. For the purpose of the group-level analysis, registration of low-resolution functional images to the corresponding high-resolution structural images was performed for each subject (Jenkinson and Smith, 2001), and followed by registration to a standard brain (MNI template, Collins et al., 1994). The raw Z statistic images from the group analysis were thresholded at Z scores >2.3. A cluster-based approach (threshold $p<0.05$) was used to correct for multiple comparisons (Worsley et al., 1992).

Single-subject analysis

As the quality of the EPI scans was high enough to recognize necessary anatomical landmarks, no image coregistration procedures were applied in this analysis, not even the alignment of functional to structural scans was necessary to assign activations to the ROIs chosen.

Single subject data were initially thresholded at Z = 2.3 and cluster corrected (minimum number of contiguous voxels constituting a cluster > 4). For each subject, the coordinates of the voxel with the highest Z score (i.e. most significantly activated) in each of the 8 ROIs (directly identified on the non-normalized functional images) were noted. This way, significant activations were found in 344/352 ROI analyses (11 subjects x 8 regions of interest x 4 conditions = 352 analyses). Lowering the statistical threshold to Z = 2 .0 yielded

two additional activations. The whole procedure of identification of the peak voxel within each of the ROIs was done separately by two experimenters (UB and GDI) to double-check the results. The few cases (11 out of 346) where different locations had been selected by these experimenters were re-examined until agreement regarding the location of the peak voxel was reached.

To check for the presence of hand-foot somatotopy, differences in coordinates (x, y, z) between hand and foot peak Z-score activation were calculated for each subject. Significance was tested using paired Student's t-tests separately for x, y and z coordinates (in mm) for all subjects; presence of somatotopy was assumed in cases where the difference between hand and foot peak activations within an ROI was significantly larger than 0 mm for at least one axis. Differences in location below 2 mm in the horizontal plane and 4 mm in vertical direction were not considered as valid even in case they were significant, because this was below the scanning resolution (2x2x4 mm). Differences in the location of activations induced by the two stimulation modalities (heat or pin prick) within the same stimulation area (hand or foot) were tested using the same approach.

Results

Pain ratings

During the fMRI experiment the average pricking pain intensity ratings (on 0 to 10 scale) were as follows: laser hand = 2.8 ±1.1; laser foot = 3.2 ±1.3; pin prick hand = 1.7 ±0.7; pin prick foot = 2.1 ±0.7. Two-way ANOVA revealed a significant main effect of the modality (higher pain ratings for laser stimulation compared to pin prick stimulation; $p<0.01$), no significant main effect for stimulus site, and no significant interaction. Average pain ratings remained stable throughout the experiment (Kruskall-Wallis test, $p>0.3$).

272

273 ***fMRI activations***

274 ***Group analysis***

275 The initial group analysis using a significance threshold of 2.3 (cluster threshold of 4 voxels)
276 yielded significant activations in various brain areas. In Figure 3A, three transversal slices 4
277 mm apart from each other in superior-inferior (z-coordinate) direction show voxels with
278 significant activations (z-score >2.3, see color bars) following stimulation of the hand or foot
279 with laser (LH, laser hand; LF, laser foot) or pinprick stimuli (PH, pin prick hand; PF, pin
280 prick foot). At a glance, there is a scattering of voxels visible without clear hand-foot
281 somatototopy within the operculo-insular and frontal regions, with the widest distribution for
282 laser hand stimulation (upper row) and the smallest number of significant voxels for pin prick
283 foot stimulation (bottom row). The area which is active most reliably in all of the 4
284 modalities (laser hand, laser foot, pinprick hand, pinprick foot) is the posterior insula of the
285 left (contralateral) hemisphere. On the right panel, Figure 3B, hand and foot stimulation is
286 shown on the same brain slice for laser (top) and pin prick stimulation (bottom). The
287 significance threshold was raised from 2.3 to 3.8, which unmasks a different representation
288 for hand and foot in the posterior insula. The hand representation (red voxels for laser, dark
289 blue voxels for pinprick stimuli) is shown to be anterior to the foot representation (orange
290 voxels for laser, light blue voxels for pinprick stimuli; white voxels: overlap).

291

292 ***Single subject ROI analysis***

293 The quality of the functional EPI scans was high enough to localize peak activations within
294 each of the 8 ROIs in almost every case (346 of 352 analyses). The peak Z-scores ranged
295 from 2.2 to 8.5. Differences in location and Z scores of peak voxels for all ROIs between

locations of stimulation (hand and foot) in each of the two modalities are shown in Table I. Results for each for the single dimensions are shown separately (X: medial-lateral, Y: anterior-posterior, Z: superior-inferior) as well as in three-dimensional distance (3D). An asterisk marks significant differences.

As an example of the spatial scattering of individual cortical activations in three-dimensional space, Figure 4 illustrates the individual peak voxel activations of laser hand (red dots) and laser foot (yellow dots) stimulation within the ROI "left SII" projected into the brain of one of the participants of this study. The average localizations (large symbols) show a shift of hand and foot representation in medial-lateral direction, with the hand representation further lateral. The overlap of the distributions of red and yellow symbols demonstrates why the individual analysis with pairwise comparisons within subjects is likely to yield sharper separations with a better spatial resolution than the resolution that can be achieved by means of a group analysis.

For *heat stimulation* (Table Ia), we found a significant somatotopy in: (1) contralateral (left) SII/PV, with the hand 6.9 mm lateral to the foot, and a three-dimensional distance of the x, y and z coordinates (square root ($x^2 + y^2 + z^2$)) of 7.4 mm; (2) contralateral (left) posterior insula, with hand 8.5 mm anterior to the foot and a 3D distance of 9.1 mm; and (3) contralateral (left) anterior insula, with hand 9.3 mm anterior to the foot, and a 3D distance of 10.0 mm (Fig. 5, left panel).

For *pin prick stimulation* (Table Ib), we found a significant somatotopy only in the contralateral (left) posterior insula, with hand 4.4 mm anterior to the foot, and a 3D distance of 9.1 mm (Fig. 5, right panel).

For *hand stimulation* (Table IIa) we found a significant difference between the location of the responses to laser and pin prick stimulation in the contralateral (left) anterior insula, with the response to laser stimulation 11.0 mm anterior to the response to pin prick stimulation, and a 3D distance of 11.4 mm (Fig. 6, left panel). For *foot stimulation* (Table IIb) we could not identify significant differences between stimulation modalities. Differences in location (in mm) and Z scores of peak voxels for all ROIs between modalities of stimulation (heat and pin prick) in each ROI are shown in Table II.

In all comparisons (both between body sites and between modalities), the Z-scores were constant across subjects within the conditions tested, and the differences in Z-scores were not significantly different from zero (Tables I and II).

334 ## Discussion

335 Activation of the operculo-insular cortex has been demonstrated in the vast majority of
336 studies investigating the brain responses to nociceptive stimuli in humans (Peyron et al 2000,
337 Apkarian et al 2005). Using high-resolution fMRI based on individual, untransformed
338 anatomical and functional data, we now demonstrate a somatotopic representation of
339 nociceptive stimulation in three operculo-insular ROIs. There were spatially separate cortical
340 responses to hand and foot stimulation in the contralateral posterior insula following both
341 heat and pin prick stimulation, and in the contralateral anterior insula and parietal operculum
342 following heat stimulation only. The mediolateral somatotopy in the parietal operculum was
343 consistent with that of tactile representation in SII or PV (Disbrow et al. 2000). The posterior-
344 anterior somatotopy in the insula was consistent with the predicted somatotopy for cortical
345 projection areas of the proposed thalamic nucleus, VMpo (Craig 1995). Furthermore, we
346 found differences in location of cortical responses to heat stimulation versus pin prick
347 stimulation in contralateral anterior insula following hand stimulation, and contralateral
348 parietal operculum following foot stimulation.

349

350 ### *Specificity of nociceptive stimuli and specificity of the areas activated*

351 We can assume with enough certainty, that the stimuli applied in this study were specific to
352 activate nociceptive fibers. This is clearly the case for the laser stimulus, which has been
353 shown to activate Aδ- and C-nociceptors, only a tiny fraction of C-warm-fibers (approx.
354 10%), and no Aβ-fibers as demonstrated in single fiber recordings (Bromm and Treede 1984,
355 Bromm et al. 1984, Treede et al. 1995). The contribution of the C-warm fibers to the centrally
356 conducted signal seems negligible, since 80% of this fraction stops firing at all at

357 temperatures in the higher noxious range (45-50°C; LaMotte and Campbell 1978, Darian-
358 Smith et al 1979).

359 The pin-prick stimulus, on the other hand, is less specific for nociception, since it co-activates
360 Aβ-, Aδ- and C-fibers. Whereas the surface of the mechanical probe seems to be hardly
361 relevant to single unit responses of low threshold mechanoreceptors (Aβ-fibers), the
362 prickliness is differentially coded by a population of Aδ- and polymodal C-nociceptors
363 (Garnsworthy et al. 1988). Among these, probe size (diameter) and force are better reflected
364 in activity of Aδ- than in activity of C-nociceptors with one sub-population having high
365 discharge rates at the threshold where mechanical stimuli are just recognized as sharp, and
366 another sub-population with high discharge rates at higher intensities (Greenspan and
367 McGillis 1994, Garell et al 1996).

368 Taken together, the stimulation used in our study was nociceptive, and thus, the brain areas
369 activated, like the frontal operculum, SII/PV, and anterior and posterior insula (and other
370 regions outside our ROIs) were responsive to noxious stimuli. Since we did not compare
371 brain responses following noxious versus non-noxious stimulation in this study, we cannot
372 conclude directly that these brain areas are, in turn, specific for nociceptive processing. The
373 fact that for tactile stimuli so far only a lateral-medial representation has been identified in
374 the area of SII/PV suggests, that the double anterior-posterior somatotopy in the insula might
375 be specific for nociception. On the other hand, there is evidence for polymodality of regions
376 within the operculo-insular cortex coming from a number of studies (Davis et al. 1998,
377 Downar et al. 2000, Matsuhashi et al. 2004).

378

379 ***Somatotopy in the opercular cortex***

380 In functional imaging studies of the human brain, usually the entire parietal operculum and
381 sometimes even parts of the frontal operculum are labelled SII. According to electro-
382 physiological and imaging studies in monkeys and humans of the parietal operculum
383 (Krubitzer et al. 1995, Disbrow et al. 2000, Fitzgerald et al. 2004), this large area can be
384 separated into two or three functionally distinct regions with separate representations of the
385 body: PV (anterior part, facing the posterior insula), SII proper (more posterior than PV), and
386 possibly a third area further posterior. Cytoarchitectonically, the human parietal opercular
387 region has recently been divided into four areas (OP1 – OP4, Eickhoff et al. 2006a), where
388 OP1 corresponds to SII and OP4 to PV. A meta-analysis of imaging studies investigating the
389 responses to nociceptive and non-nociceptive stimuli found the clusters responding to
390 nociceptive stimuli within OP1, the posterior part of the parietal operculum (Eickhoff et al
391 2006b), and the clusters responding to non-nociceptive stimuli more anterior, at the border of
392 OP1 and OP4. The fMRI peaks within the posterior operculum (SII/PV) as identified in the
393 single subject analysis of the present study (Table 1, Fig. 5) were located mostly in OP1 or at
394 the border of OP1 and OP4, and thus are consistent with being in SII proper.

395

396 The somatotopy that we found in SII is consistent with that known for tactile representation
397 in SII (Disbrow et al. 2000). A similar somatotopy, with hand representation lateral to foot
398 representation in SII, had previously been reported in a fMRI study using laser stimulation
399 (Bingel et al 2004). However, possibly due to the limited spatial resolution, they were not
400 able to ascertain whether the peak of activity following foot stimulation was located in SII or
401 posterior insula. We found distinct locations for foot representation both in SII proper and
402 posterior insula and hence demonstrated the presence of a nociceptive homunculus for
403 thermal stimuli in SII. Ferretti et al (2004) found two activation areas for hand and foot in
404 SII/PV; within each activation area, nociceptive stimuli were represented more posteriorly

405 than non-nociceptive stimuli. These authors reported a significant somatotopy for the non-
406 nociceptive stimuli only; however, they used two different intensities of electrical
407 stimulation, and brain responses were detected using a 1.5 T scanner, thus raising the
408 questions of specificity of the afferent neuronal populations activated and spatial resolution of
409 the imaging technique. Our data indicate that apart from tactile information, as has been
410 demonstrated by other investigators (Disbrow et al. 2000, Ferretti et al. 2004), also
411 nociceptive information is projecting to SII as part of the "classical" lateral pain pathway and
412 is somatotopically organized.
413

414 Only few nociceptive neurons have been identified in SII proper (Robinson and Burton
415 1980), and the largest published series of nociceptive neurons in that region is from a more
416 posterior area (Dong et al. 1989). The scarcity of monkey electrophysiological data may be
417 due to inadequate search stimuli: both type I and II AMH are not activated by gentle
418 mechanical search stimuli, and electrical stimulation is necessary to study these primary
419 afferents (Treede et al. 1998).
420

421 Although in the frontal operculum we observed significant responses to the nociceptive
422 stimulation, we did not find significant hand-foot somatotopy in this area. We could thus not
423 reproduce the posterior-anterior somatotopy in the frontal operculum observed by Vogel and
424 coworkers (Vogel et al. 2003). One possible explanation could be that in that their source
425 analysis study, the somatotopy of the dorsal insula was projected into the operculum. On the
426 other hand, invasive depth recordings have confirmed a generator source within the frontal
427 operculum, so this generator may be non-somatotopically organized.
428

429 ***Somatotopy in the insular cortex***

430 As there is not yet an established standard on how to segregate the insula into functionally
431 different ROIs, we chose to use gross anatomical features. The separation into an anterior
432 part, containing the 3 short gyri, and a posterior part, containing the 2 long gyri, separated by
433 the central insular sulcus, has been used previously by Ostrowsky et al. (2000) during
434 invasive mapping and by Bense et al. (2001) in an fMRI study. Efforts to establish a
435 stereotactic template of the insula have also been made (Afif et al. 2009). According to
436 Brodmann (1909), the human insula contains a dorsogranular field and a ventrorostral
437 agranular field, however, he did not assign any area numbers to it. Furthermore, monkey data
438 show different cytoarchitecture between anterior and posterior insula, possibly with three
439 distinct subregions (Augustine 1985). Very recently, first data on cytoarchitectonic mapping
440 of the human posterior insula obtained from analysis of post mortem brains has become
441 available (Kurth et al. 2009). These data suggest an even finer separation of the insula than
442 previously supposed, but this work is currently still in progress.

443

444 We found two separate representations in the insula, both with the posterior-anterior
445 somatotopy predicted for VMpo projection areas. A similar somatotopy with hand
446 representation anterior to foot representation in dorsal posterior insula had previously been
447 reported in a fMRI study using contact heat stimulation (Brooks et al 2005) and was very
448 recently demonstrated by an intra-operative stimulation study using laser stimuli (Mazzola et
449 al. 2009). Another study with painful stimulation of muscles also reported hand
450 representation anterior and lateral of foot in dorsal posterior insula (Henderson et al. 2007).

451

452 These data underline the importance of the (posterior) insular cortex as a projection target for
453 the spinothalamic pathway through lamina 1 and the proposed VMpo thalamic nucleus (Craig
454 and Zhang 2006). In addition to the previous studies, we found the same anterior-posterior
455 gradient of hand and foot representation in both parts (anterior and posterior) of the
456 contralateral (left) insula. In response to pin prick stimuli a similar somatotopical
457 organization was found in the same direction within the posterior insula. If one follows the
458 suggestion by Craig (2009b), this somatotopy in the posterior insula could be a VMpo
459 projection with re-representation in the anterior part of the insula.

460

461 The findings of enhanced activity of the left frontal operculo-insular cortex during a
462 discrimination task using EEG source analysis (Schlereth et al. 2003) and increased activity
463 of the anterior insula (bilaterally) during a memory task of intensity discrimination using
464 fMRI (Albanese et al. 2007) following hand stimulation, supports the finding of hand-foot
465 somatotopy in this region since stimulus discrimination requires an anatomical map of the
466 body.

467

468 ***Separate representation of noxious heat and pin prick stimuli in the anterior insula?***

469 An unexpected finding was the significantly different representation of noxious heat and pin
470 prick stimulation of the hand in the anterior insular cortex, with heat pain representation
471 located on average 11mm more anterior compared to the representation of mechanical pain.
472 We did not observe the same phenomenon for stimulation of the foot. One possible
473 explanation could be that a larger hand representation yields stronger fMRI activations,
474 making it easier to detect differences. However this seems implausible, since z-scores

475 between hand and foot activations differed less than 0.5 and were non-significant (Tables
476 1A&B), and pain ratings were even slightly lower following hand stimulation.
477
478 The anterior part of the insula has been assigned to the processing of emotion as well as pain
479 anticipation and human awareness (Craig 2009a, Damasio et al. 2000, Ploghaus et al. 1999).
480 It has been further characterized as center for interoception that integrates somato-visceral
481 input from the body together with autonomic input and emotional awareness to drive
482 adequate behavioural and motor responses (Craig 2009b, Critchley 2005). Different self-
483 induced emotions, mostly negative, lead to different activations within the anterior insulas
484 (left and right; Damasio et al. 2000). Although the subjects in our study had to rate the
485 pricking aspect of the evoked pain sensation which better emphasizes the sensory than the
486 affective dimension, since sensory and affective pain dimensions are closely interrelated, one
487 may speculate that the interoceptive input is different with the result of different
488 representations within the anterior insula for noxious heat and mechanical stimuli. The
489 different representation of heat pain could be due to different levels of attention, emotion, or
490 anticipation induced by a higher level of potential threat or negative affect associated with the
491 laser stimulus. Since sensory inputs from the hands are more important than from the feet in
492 everyday-life, and it appears reasonable why we found this segregation for the hands only.
493

494 ***Conclusion***

495 By evaluating four subregions of the operculo-insular cortex separately we identified at least
496 three representations of nociceptive inputs within this region. We have therefore contributed
497 to a resolution of a controversy in the previously published literature that tried to establish the
498 single representation of pain in that region. Our data indicate that both the classical lateral

499 pain pathway from VPI to SII, as well as the pathway from VMpo to dorsal posterior insula
500 have cortical projections that are somatotopically organized, but at 90° angle from each other.
501 Due to the limited temporal resolution of fMRI it was not possible to ascertain whether the
502 projection target in the anterior insula is processing information in parallel to the posterior
503 insula or is activated following the posterior part in a sequential way.

504

505 **Acknowledgements**

506 This study was supported by the Deutsche Forschungsgemeinschaft (DFG Tr 236/13-3). GDI
507 is University Research Fellow of The Royal Society. FMRIB Centre is supported by the
508 Medical Research Council of Great Britain.

509

References

Afif A, Hoffmann D, Minotti L, Benabid AL, Kahane P. Middle short gyrus of the insula implicated in pain processing. Pain 138: 546-55, 2008.

Afif A, Hoffmann D, Becq G, Guenot M, Magnin M, Mertens P. MRI-Based Definition of a Stereotactic Two-Dimensional Template of the Human Insula. Stereotact Funct Neurosurg. 87: 385-394, 2009.

Albanese MC, Duerden EG, Rainville P, Duncan GH. Memory traces of pain in human cortex. J Neurosci. 27: 4612-4620, 2007.

Andersson JLR, Lilja A, Hartvig P, Långström B, Gordh T, Handwerker H, Torebjörk E. Somatotopic organization along the central sulcus, for pain localization in humans, as revealed by positron emission tomography. Exp Brain Res 117: 192-199, 1997.

Apkarian AV, Bushnell C, Treede RD, Zubieta JK. Human brain mechanisms of pain perception and regulation in health and disease. Eur J Pain 9: 463-484, 2005.

Augustine JR (1985) The insular lobe in primates including humans. Neurol Res 7:2-10.

Baumgärtner U, Buchholz HG, Bellosevich A, Magerl W, Siessmeyer T, Rolke R, Höhnemann S, Piel M, Rösch F, Wester HJ, Henriksen G, Stoeter P, Bartenstein P, Treede RD, Schreckenberger M. High opiate receptor binding potential in the human lateral pain system. NeuroImage 30: 692-699, 2006a.

Baumgärtner U, Magerl W, Klein T, Hopf HC, Treede R-D. Neurogenic hyperalgesia versus painful hypoalgesia: two distinct mechanisms of neuropathic pain. Pain 96: 141-151, 2002.

Baumgärtner U, Tiede W, Treede R-D, Craig AD. Laser-evoked potentials are graded and somatotopically organized anteroposteriorly in the operculoinsular cortex of anesthetized monkeys. J Neurophysiol 96: 2802-2808, 2006b.

Bense S, Stephan T, Yousry TA, Brandt T, Dieterich M. Multisensory cortical signal increases and decreases during vestibular galvanic stuimulation (fMRI). J Neurophysiol 85: 886-899, 2001.

Bingel U, Lorenz J, Glauche V, Knab R, Gläscher J, Weiller C, Büchel C. Somatotopic organization of human somatosensory cortices for pain: a single trial fMRI study. Neuroimage 23: 224-232, 2004.

Brodmann K. Vergleichende Lokalisationslehre der Grosshirnrinde in ihren Prinzipien dargestellt auf Grund des Zellenbaues. Barth, Leipzig, 1909.

Bromm B, Jahnke MT, Treede RD. Responses of human cutaneous afferents to CO2 laser stimuli causing pain. Exp Brain Res 55: 158-166, 1984.

Bromm B, Treede RD. Nerve fibre discharges, cerebral potentials and sensations induced by CO2 laser stimulation. Hum Neurobiol 3: 33-40, 1984.

Brooks JC, Zambreanu L, Godinez A, Craig AD, Tracey I. Somatotopic organisation of the human insula to painful heat studied with high resolution functional imaging. Neuroimage 27: 201-209, 2005.

Collins DL, Neelin P, Peters TM, Evans AC. Automatic 3D intersubject registration of MR volumetric data in standardized Talairach space. J Comput Assist Tomogr 18: 192-205, 1994.

Craig AD. Emotional moments across time: a possible neural basis for time perception in the anterior insula. Philos Trans R Soc Lond B Biol Sci 364: 1933-1942, 2009a.

Craig AD. How do you feel--now? The anterior insula and human awareness. Nat Rev Neurosci 10: 59-70, 2009b.

Craig AD. Supraspinal projections of lamina I neurons. In: Forebrain Areas Involved in Pain Processing. Edited by Besson J-M, Guilbaud GOH. Paris: John Libbey; 1995: 13-26.

Craig AD, Bushnell MC, Zhang ET, Blomqvist A. A thalamic nucleus specific for pain and temperature sensation. Nature 372: 770-773, 1994.

Craig AD, Dostrovsky JO. Processing of nociceptive information at supraspinal levels. In: Anesthesia: Biologic Foundations, edited by T.L.Yaksh. Philadelphia, PA: Lippincott-Raven Publishers, 1997, p. 625-642.

Craig AD, Zhang ET. Retrograde analyses of spinothalamic projections in the macaque monkey: input to posterolateral thalamus. J Comp Neurol 499: 953-964, 2006.

Critchley HD. Neural mechanisms of autonomic, affective, and cognitive integration. J Comp Neurol 493:154-166, 2005.

Cruccu G, Pennisi E, Truini A, Iannetti GD, Romaniello A, Le Pera D, De Armas L, Leandri M, Manfredi M, Valeriani M. Unmyelinated trigeminal pathways as assessed by laser stimuli in humans. Brain 126: 1-11, 2003.

Damasio AR, Grabowski TJ, Bechara A, Damasio H, Ponto LL, Parvizi J, Hichwa RD. Subcortical and cortical brain activity during the feeling of self-generated emotions. Nat Neurosci 3: 1049-1056, 2000.

Darian-Smith I, Johnson KO, LaMotte C, Shigenaga Y, Kenins P, Champness P. Warm fibers innervating palmar and digital skin of the monkey: responses to thermal stimuli. J Neurophysiol 42: 1297-1315, 1979.

DaSilva AF, Becerra L, Makris N, Strassman AM, Gonzalez RG, Geatrakis N, Borsook D. Somatotopic activation in the human trigeminal pain pathway. J Neurosci 22: 8183-8192, 2002.

Davis KD, Kwan CL, Crawley AP, Mikulis DJ. Functional MRI study of thalamic and cortical activations evoked by cutaneous heat, cold, and tactile stimuli. J Neurophysiol 80: 1533-1546, 1998.

Disbrow E, Roberts T, Krubitzer L. Somatotopic organization of cortical fields in the lateral sulcus of homo sapiens: evidence for SII and PV. J Comp Neurol 418: 1-21, 2000.

Dong WK, Salonen LD, Kawakami Y, Shiwaku T, Kaukoranta EM, Martin RF. Nociceptive responses of trigeminal neurons in SII-7b cortex of awake monkeys. Brain Res 484: 314-324, 1989.

Downar J, Crawley AP, Mikulis DJ, Davis KD. A multimodal cortical network for the detection of changes in the sensory environment. Nat Neurosci 3:277-283, 2000.

Dum RP, Levinthal DJ, Strick PL. The spinothalamic system targets motor and sensory areas in the cerebral cortex of monkeys. J Neurosci 29:14223-35, 2009.

Eickhoff SB, Schleicher A, Zilles K, Amunts K. The human parietal operculum. I. Cytoarchitectonic mapping of subdivisions. Cereb Cortex 16: 254-267, 2006a.

Eickhoff SB, Amunts K, Mohlberg H, Zilles K. The human parietal operculum. II. Stereotaxic maps and correlation with functional imaging results. Cereb Cortex 16: 268-279, 2006b.

Ferretti A, Del Gratta C, Babiloni C, Caulo M, Arienzo D, Tartaro A, Rossini PM, Romani GL. Functional topography of the secondary somatosensory cortex for nonpainful and painful stimulation of median and tibial nerve: an fMRI study. Neuroimage 23: 1217-1225, 2004.

Fitzgerald PJ, Lane JW, Thakur PH, and Hsiao SS. Receptive field properties of the macaque second somatosensory cortex: evidence for multiple functional representations. J Neurosci 24: 11193-11204, 2004.

Frot M, Mauguière F. Dual representation of pain in the operculo-insular cortex in humans. Brain 126: 438-450, 2003.

Garell PC, McGillis SL, Greenspan JD. Mechanical response properties of nociceptors innervating feline hairy skin. J Neurophysiol 75: 1177-1189, 1996.

Garnsworthy RK, Gully RL, Kenins P, Mayfield RJ, Westerman RA. Identification of the physical stimulus and the neural basis of fabric-evoked prickle. J Neurophysiol 59: 1083-1097, 1988.

Gelnar PA, Krauss BR, Szeverenyi NM, and Apkarian AV. Fingertip representation in the human somatosensory cortex: An fMRI study. Neuroimage 7: 261-283, 1998.

Greenspan JD and McGillis SLB. Thresholds for the perception of pressure, sharpness, and mechanically evoked cutaneous pain: Effects of laterality and repeated testing. Somatosens Motor Res 11: 311-317, 1994.

Greenspan JD, Thomadaki M, McGillis SLB. Spatial summation of perceived pressure, sharpness and mechanically evoked cutaneous pain. Somatosens Motor Res 14: 107-112, 1997.

Greenspan JD, Lee RR, Lenz FA. Pain sensitivity alterations as a function of lesion location in the parasylvian cortex. Pain 81: 273-282, 1999.

Head H, Holmes G. Sensory disturbances from cerebral lesions. Brain 34: 102-254, 1911.

Henderson LA, Gandevia SC, Macefield VG. Somatotopic organization of the processing of muscle and cutaneous pain in the left and right insula cortex: a single-trial fMRI study. Pain. 128: 20-30, 2007.

Iannetti GD, Truini A, Romaniello A, Galeotti F, Rizzo C, Manfredi M, Cruccu G. Evidence of a specific spinal pathway for the sense of warmth in humans. J Neurophysiol 89: 562-570, 2003.

Iannetti GD, Leandri M, Truini A, Zambreanu L, Cruccu G, Tracey I. A-delta nociceptor response to laser stimuli: selective effect of stimulus duration on skin temperature, brain potentials and pain perception. Clin Neurophysiol 115: 2629-2637, 2004.

Iannetti GD Zambreanu L, Cruccu G, Tracey I. Operculoinsular cortex encodes pain intensity at the earliest stages of cortical processing: a study with laser evoked potentials in humans. Neuroscience 131(1):199-208, 2005.

Jenkinson M, Bannister P, Brady M, Smith S. Improved optimization for the robust and accurate linear registration and motion correction of brain images. Neuroimage 17: 825-841, 2002.

Jenkinson M, Smith S. A global optimisation method for robust affine registration of brain images. Med Image Anal 5: 143-156, 2001.

Kaas JH. What, if anything, is SI? Organization of first somatosensory area of cortex. Physiol Rev 63: 206-231, 1983.

Krubitzer L, Clarey J, Tweedale R, Elston G, Calford M. A redefinition of somatosensory areas in the lateral sulcus of macaque monkeys. J Neurosci 15: 3821-3839, 1995.

Kurth F, Eickhoff SB, Schleicher A, Hoemke L, Zilles K, Amunts K. Cytoarchitecture and Probabilistic Maps of the Human Posterior Insular Cortex. Cereb Cortex 2009 [Epub ahead of print]

LaMotte RH, Campbell JN. Comparison of responses of warm and nociceptive C-fiber afferents in monkey with human judgments of thermal pain. J Neurophysiol 41: 509-528, 1978.

Lenz FA, Dostrovsky JO, Tasker RR, Yamashiro K, Kwan HC, Murphy JT. Single-unit analysis of the human ventral thalamic nuclear group: somatosensory responses. J Neurophysiol 59: 299-316, 1988.

Lenz FA, Dougherty PM. Pain processing in the human thalamus. In: Thalamus. Experimental/Clinical Aspects, Vol. II, edited by Steriade M, Jones EG, McCormick DA. Oxford, UK: Elsevier Press, 1997, p. 617-651.

Lenz FA, Kwan HC, Martin R, Tasker R, Richardson RT, Dostrovsky JO. Characteristics of somatotopic organization and spontaneous neuronal activity in the region of the thalamic principal sensory nucleus in patients with spinal cord transection. J Neurophysiol 72: 1570-1587, 1994.

Magerl W, Fuchs PN, Meyer RA, and Treede RD. Roles of capsaicin-insensitive nociceptors in pain and secondary hyperalgesia. Brain 124: 1754-1764, 2001.

Matsuhashi M, Ikeda A, Ohara S, Matsumoto R, Yamamoto J, Takayama M, Satow T, Begum T, Usui K, Nagamine T, Mikuni N, Takahashi J, Miyamoto S, Fukuyama H, Shibasaki H. Multisensory convergence at human temporo-parietal junction - epicortical recording of evoked responses. Clin Neurophysiol 115: 1145-1160, 2004.

Mazzola L, Isnard J, Peyron R, Guénot M, Mauguière F. Somatotopic organization of pain responses to direct electrical stimulation of the human insular cortex. Pain.146: 99-104, 2009.

Özcan M, Baumgärtner U, Vucurevic G, Stoeter P, Treede RD. Spatial resolution of fMRI in the human parasylvian cortex: comparison of somatosensory and auditory activation. Neuroimage 25: 877-887, 2005.

Ostrowsky K, Isnard J, Ryvlin P, Guenot M, Fischer C, Mauguiere F. Functional mapping of the insular cortex: clinical implication in temporal lobe epilepsy. Epilepsia 41: 681-686, 2000.

Ostrowsky K, Magnin M, Ryvlin P, Isnard J, Guenot M, Mauguière F. Representation of pain and somatic sensation in the human insula: a study of responses to direct electrical cortical stimulation. Cereb Cortex 12: 376-385, 2002.

Peyron R, Laurent B, García-Larrea L. Functional imaging of brain responses to pain. A review and meta-analysis. Neurophysiol Clin 30: 263-288, 2000.

Ploghaus A, Tracey I, Gati JS, Clare S, Menon RS, Matthews PM, Rawlins JN. Dissociating pain from its anticipation in the human brain. Science 284: 1979-1981, 1999.

Ploner M, Schmitz F, Freund HJ, Schnitzler A. Parallel activation of primary and secondary somatosensory cortices in human pain processing. J Neurophysiol 81: 3100-3104, 1999.

Rios M, Treede RD, Lee JI, Lenz FA. Direct evidence of nociceptive input to human anterior cingulate gyrus and parasylvian cortex. Curr Rev Pain 3: 256-264, 1999.

Robinson CJ and Burton H. Somatic submodality distribution within the second somatosensory (SII), 7b, retroinsular, postauditory, and granular insular cortical areas of M. fascicularis. J Comp Neurol 192: 93-108, 1980.

Rolke R, Baron R, Maier C, Tölle TR, Treede RD, Beyer A, Binder A, Birbaumer N, Birklein F, Botefur IC, Braune S, Flor H, Huge V, Klug R, Landwehrmeyer GB, Magerl W, Maihöfner C, Rolko C, Schaub C, Scherens A, Sprenger T, Valet M, Wasserka B. Quantitative sensory testing in the german research network on neuropathic pain (DFNS): standardized protocol and reference values. Pain 123: 231-243, 2006.

Schlereth T, Baumgärtner U, Magerl W, Stoeter P, Treede R-D. Left-hemisphere dominance in early nociceptive processing in the human parasylvian cortex. Neuroimage 20: 441-454, 2003.

Slugg RM, Meyer RA, Campbell JN. Response of cutaneous A- and C-fiber nociceptors in the monkey to controlled-force stimuli. J Neurophysiol 83: 2179-2191, 2000.

Tarkka IM and Treede RD. Equivalent electrical source analysis of pain-related somatosensory evoked potentials elicited by a CO2 laser. J Clin Neurophysiol 10: 513-519, 1993.

Tracey I, Mantyh PW. The cerebral signature for pain perception and its modulation. Neuron 55: 377-391, 2007.

Treede RD, Apkarian AV, Bromm B, Greenspan JD, Lenz FA. Cortical representation of pain: functional characterization of nociceptive areas near the lateral sulcus. Pain 87: 113-119, 2000.

Treede RD, Meyer RA, Campbell JN. Myelinated mechanically insensitive afferents from monkey hairy skin: heat-response properties. J Neurophysiol 80: 1082-1093, 1998.

Treede R-D, Meyer RA, Raja SN, Campbell JN. Evidence for two different heat transduction mechanisms in nociceptive primary afferents innervating monkey skin. J Physiol 483: 747-758, 1995.

Vogel H, Port JD, Lenz FA, Solaiyappan M, Krauss G, Treede RD. Dipole source analysis of laser-evoked subdural potentials recorded from parasylvian cortex in humans. J Neurophysiol 89: 3051-3060, 2003.

Woolrich MW, Ripley BD, Brady M, Smith SM. Temporal autocorrelation in univariate linear modeling of fMRI data. Neuroimage 14: 1370-1386, 2001.

Worsley KJ, Evans AC, Marrett S, Neelin P. A three-dimensional statistical analysis for CBF activation studies in human brain. J Cereb Blood Flow Metab 12: 900-918, 1992.

Worsley KJ, Friston KJ. Analysis of fMRI time-series revisited - again. Neuroimage 2: 173-181, 1995.

Xu X, Fukuyama H, Yazawa S, Mima T, Hanakawa T, Magata Y, Kanda M, Fujiwara N, Shindo K, Nagamine T, Shibasaki H. Functional localization of pain perception in the human brain studied by PET. Neuroreport 8: 555-559, 1997.

Young JP, Herath P, Eickhoff S, Choi J, Grefkes C, Zilles K, Roland PE. Somatotopy and attentional modulation of the human parietal and opercular regions. J Neurosci 24: 5391-5399, 2004.

Ziegler EA, Magerl W, Meyer RA, Treede R-D. Secondary hyperalgesia to punctate mechanical stimuli: Central sensitization to A-fibre nociceptor input. Brain 122: 2245-2257, 1999.

Table 1. Differences in location and Z-scores of fMRI responses to hand and foot stimulation.

A. Laser stimulation

	Left SII	Right SII	Left PI	Right PI	Left AI	Right AI	Left FOP	Right FOP
x (mm)	6.9*	-5.0	2.2*	-2.0	0.9	0.4	3.0	2.5
y (mm)	-2.4	-5.2	8.5*	4.6	9.3*	4.0	-8.2	2.9
z (mm)	1.1	0.0	-2.2	-2.4*	-3.6	-3.3	1.2	2.5
3D (mm)	7.4	7.2	9.1	5.6	10.0	5.2	8.8	4.6
Z-score	0.2	-0.6	-1.2	-0.8	-0.4	-0.3	-0.5	-0.4

Note – all differences are obtained by subtracting the foot values from the hand values; stimuli were delivered to the right side of the body; * indicates $p < 0.05$ (paired t test).

B. Pin prick stimulation

	Left SII	Right SII	Left PI	Right PI	Left AI	Right AI	Left FOP	Right FOP
x (mm)	1.3	-4.2	0.9	-0.2	0.4	1.1	-0.9	3.2
y (mm)	-0.5	-5.8	8.9*	5.6	-2.6	4.7	0.4	-2.2
z (mm)	-0.4	2.5	-1.5	-1.8	-1.6	-2.9	-4.0	-0.8
3D (mm)	1.4	7.6	9.1	5.9	3.1	5.7	4.1	4.0
Z-score	0.5	0.1	-0.4	-0.4	0.5	0.1	0.8	0.7

Note – all differences are obtained by subtracting the foot values from the hand values; stimuli were delivered to the right side of the body; * indicates $p < 0.05$ (paired t test).

Table 2. Differences in location and Z-scores of fMRI responses to laser and pin prick stimulation.

A. Hand stimulation

	Left SII	Right SII	Left PI	Right PI	Left AI	Right AI	Left FOP	Right FOP
x (mm)	0.2	-0.2	-0.9	1.3	-0.4	-1.5	1.4	-0.6
y (mm)	0.5	-1.5	-1.5	-0.5	-11.0*	0.7	5.2	-3.6
z (mm)	1.5	-1.8	0.4	1.1	-2.8	-0.7	0.4	-1.2
3D (mm)	1.6	2.3	1.8	1.8	11.4	1.8	5.4	3.8
Z-score	-0.4	-0.2	0.0	0.1	-0.3	-0.2	0.3	0.4

Note – all differences are obtained by subtracting the laser values from the pin prick values; stimuli were delivered to the right side of the body; * indicates $p < 0.05$ (paired t test).

B. Foot stimulation

	Left SII	Right SII	Left PI	Right PI	Left AI	Right AI	Left FOP	Right FOP
x (mm)	-5.5[§]	-0.8	-2.2	2.2	1.3	0.7	-1.1	0.0
y (mm)	1.3	-0.4	-1.8	-1.0	0.0	0.0	-2.9	-1.0
z (mm)	0.0	0.4	1.1	2.4	-1.8	0.4	1.8	-3.2
3D (mm)	5.6	1.0	3.0	3.4	2.2	0.8	3.6	3.4
Z-score	0.0	0.2	0.8	0.5	0.5	0.7	0.9	0.7

Note – all differences are obtained by subtracting the laser values from the pin prick values; stimuli were delivered to the right side of the body; * indicates $p < 0.05$ (paired t test). [§] $p = 0.0508$.

836 **Captions to figures**
837
838
839
840 Figure 1: Experimental design. The figure illustrates the timing of actions performed during
841 the fMRI experiment. Laser heat and pin prick stimuli were delivered to the skin of the
842 dorsum of the hand and of the foot by an experimenter inside the scanner room. Stimuli of the
843 same modality and to the same body site were delivered in blocks of 10, with an inter-
844 stimulus interval of 11.5 s. At the end of each block, the subject was asked to provide an
845 average intensity rating for that block. The order of blocks was balanced across subjects.
846
847 Figure 2: Variability in structural anatomy and definition of regions of interest on EPI scans.
848 The left panel shows the variability in structural anatomy of the population explored in this
849 study. The individual brains were aligned to the anterior commissure (AC, origin of axes), in
850 order to display variability of structural anatomy of the insular and opercular regions on a
851 single brain. As AC is approximately located in the centre of the brain as well as of the ROIs,
852 this Talairach-like alignment was chosen to minimize the influence of inter-individual
853 anatomical differences. Each dot represents the average location of the landmarks used to
854 define the 8 regions of interest (ROIs). On each hemisphere, the medial dots indicate the
855 anterior pole of the insula, the middle of the curvature of the insula, the sulcus between the
856 3rd and 4th insular gyri (the anatomical separation of anterior and posterior insula, Bense et al
857 2001) and the posterior pole of the insula. The lateral dot indicates the location where the
858 central sulcus ends (separation between the frontal and the parietal operculum). The single
859 dot on the midline represents the posterior commissure (PC). Axis scaling is in mm, error
860 bars represent the standard error of the mean. The right panel illustrates how the 8 ROIs (in
861 yellow) were determined in a representative subject. FOP: frontal operculum; AIC: anterior
862 insular cortex; PIC: posterior insular cortex; SII: secondary somatosensory cortex

Figure 3: Group Analysis. Left (A): At the significance threshold of Z= 2.3, three transversal slices through the operculo-insular region are shown (left to right; 4 mm below AC level, 4 mm above AC level, 12 mm above AC level) in four lines for the four modalities (laser hand, laser foot, pinprick hand, pinprick foot). Although especially for the laser stimuli, the brain activations are scattered throughout the operculo-insular and frontal cortices, the brain area that is activated most consistently across the four different stimulation modalities is the left posterior insula. Right (B): Brain activation of both hand and foot stimulation is shown on the same slice (laser: top; pin prick: bottom). At an elevated threshold of Z=3.8, a differential somatotopic representation within the posterior insula in anterior-posterior direction can be seen: the hand representation is anterior to the foot representation. Top: Laser hand (red pixels) versus foot (orange pixels). Bottom: pinprick hand (dark blue) versus foot (light blue), overlapping pixels in white. Note that on group analysis level, the only somatotopic representation that can be identified is in the posterior insula. The left side of the brains is shown on the left.

Figure 4: Three-dimensional clustering of the individual cortical responses obtained within SII following laser hand (red) and foot (yellow) stimulation. To gain an impression of the variability of cortical representations within the secondary somatosensory cortex, the individual activations of all subjects (n=11) were projected onto one subject's 3D reconstruction of the brain. The individual coordinate systems were aligned to the anterior commissure and the AC-PC plane. Despite the overlap between the scatterings of the red and yellow symbols, a systematic difference in medial-lateral direction is visible, and the average localizations for hand and foot representation are illustrated by the large symbols. Grid width: 1 cm.

888

889 Figure 5: Somatotopic representation of hand and foot following noxious stimulation

890 The left panel shows the average location of the activations in response to heat (laser)
891 stimulation of the hand (red squares) and foot dorsum (orange diamonds), in each ROI. As
892 indicated by red ellipsoids, the location of the activations was significantly different (circled
893 in red) in the contralateral anterior insula, posterior insula, and parietal operculum (SII; for a
894 quantitative description of location differences see Table 1A). The right panel shows the
895 average location of the activations in response to pin prick (punctate probe) stimulation of the
896 hand (dark blue squares) and foot dorsum (pale blue diamonds), in each ROI. The location of
897 the activations was significantly different in the contralateral posterior insula (for a
898 quantitative description of location differences see Table 1B).

899 In all panels, error bars represent the standard error of the mean. The left side of the brains is
900 shown on the left. AIC: anterior insular cortex; PIC: posterior insular cortex; SII: secondary
901 somatosensory cortex

902

903 Figure 6: Different location of activations in response to heat and pin prick stimulation

904 The left panel shows the average location of the activations in response to heat (laser) and pin
905 prick (punctate probe) stimulation of the hand dorsum, in each ROI. Red squares represent
906 heat stimulation, blue squares represent pin prick stimulation. The location of the activations
907 was significantly different in the contralateral anterior insula (circled in red; AIC: anterior
908 insular cortex; for a quantitative description of location differences see Table 2A).

909 The right panel shows the average location of the activations in response to heat (laser) and
910 pin prick (punctuate probe) stimulation of the foot dorsum. Orange diamonds represent heat
911 stimulation, pale blue diamonds represent pin prick stimulation. For a quantitative description
912 of location differences see Table 2B.

In all panels error bars represent the standard error of the mean. The left side of the brains is shown on the left.

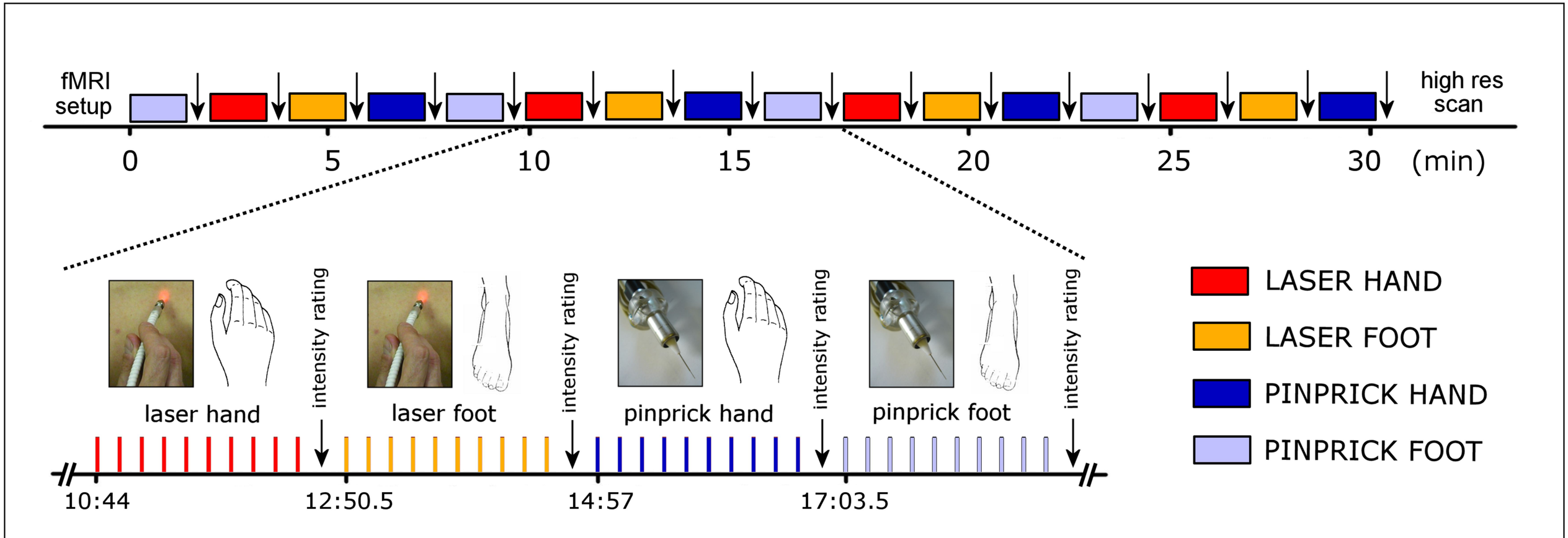
fMRI setup
high res scan
0
5
10
15
20
25
30
(min)
laser hand
intensity rating
laser foot
intensity rating
pinprick hand
intensity rating
pinprick foot
intensity rating
10:44
12:50.5
14:57
17:03.5
LASER HAND
LASER FOOT
PINPRICK HAND
PINPRICK FOOT

anatomical landmarks

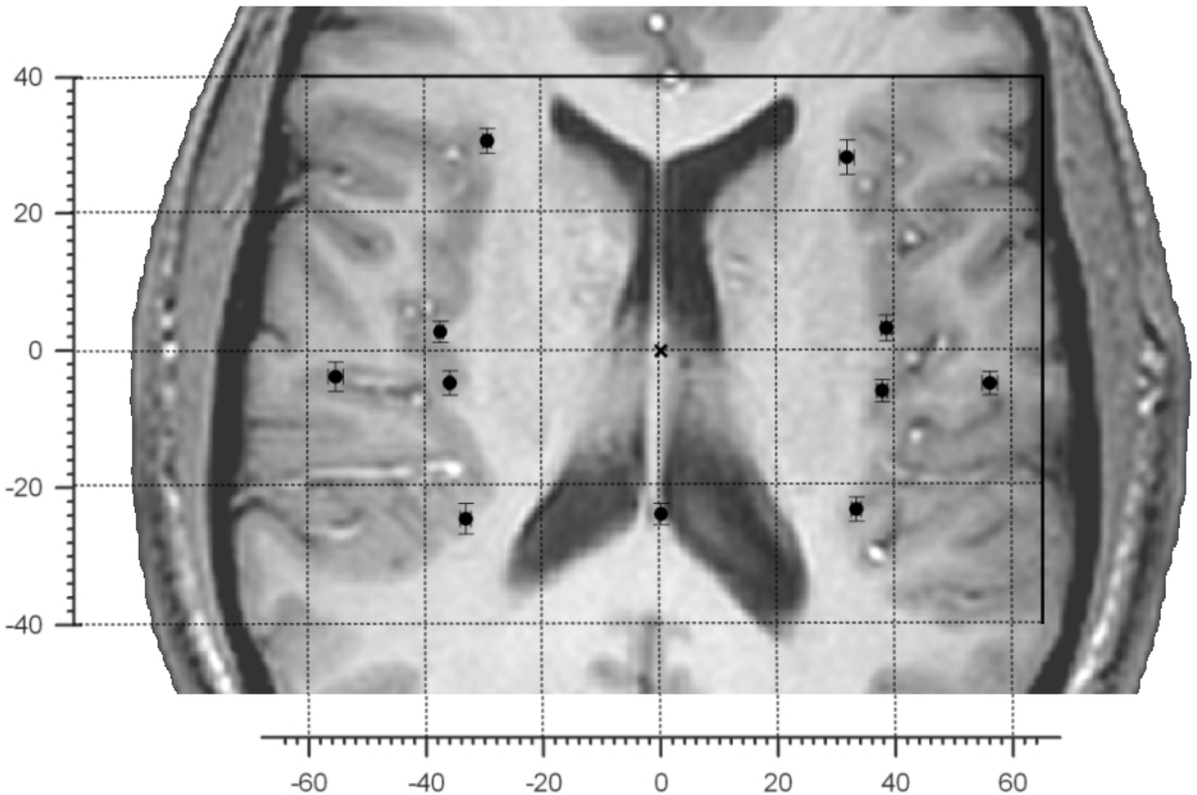

regions of interest

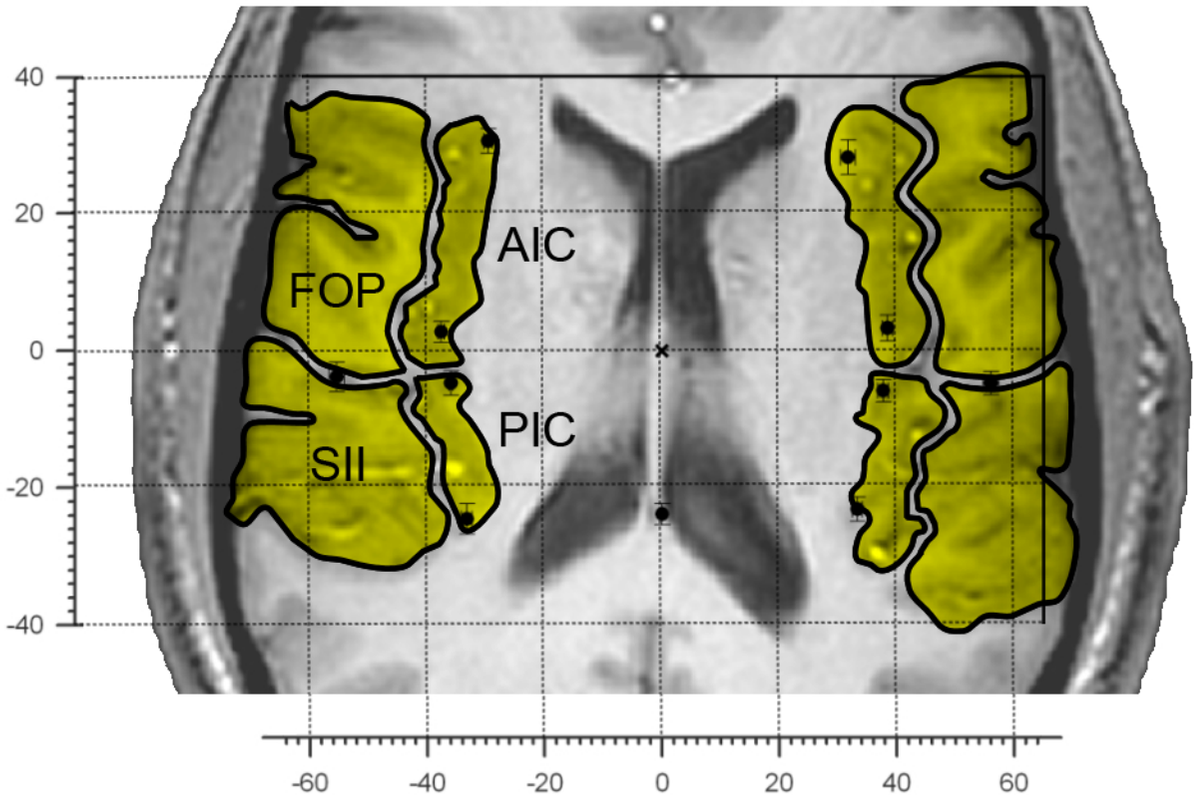

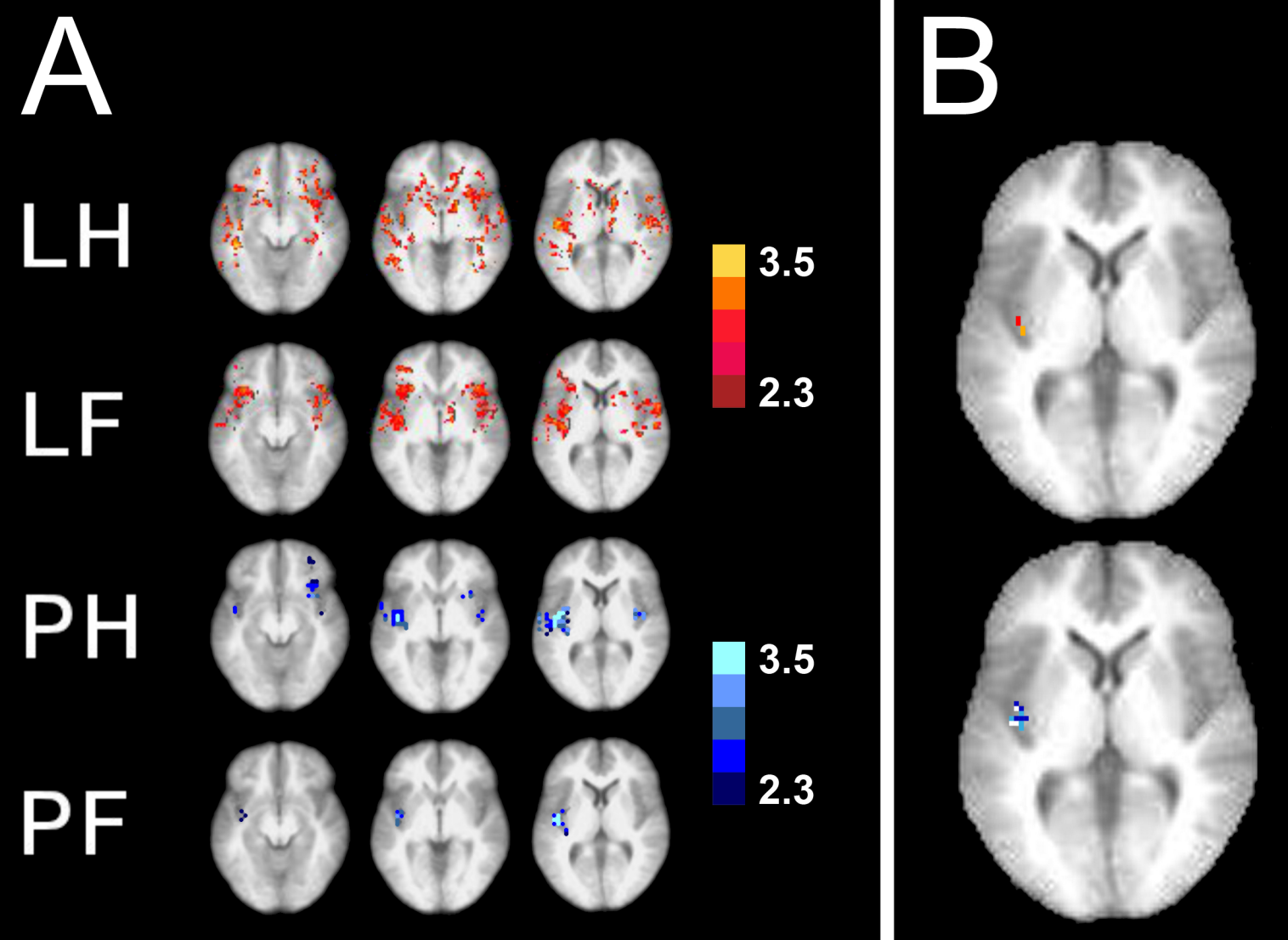
A
LH
LF
PH
PF
3.5
2.3
3.5
2.3
B

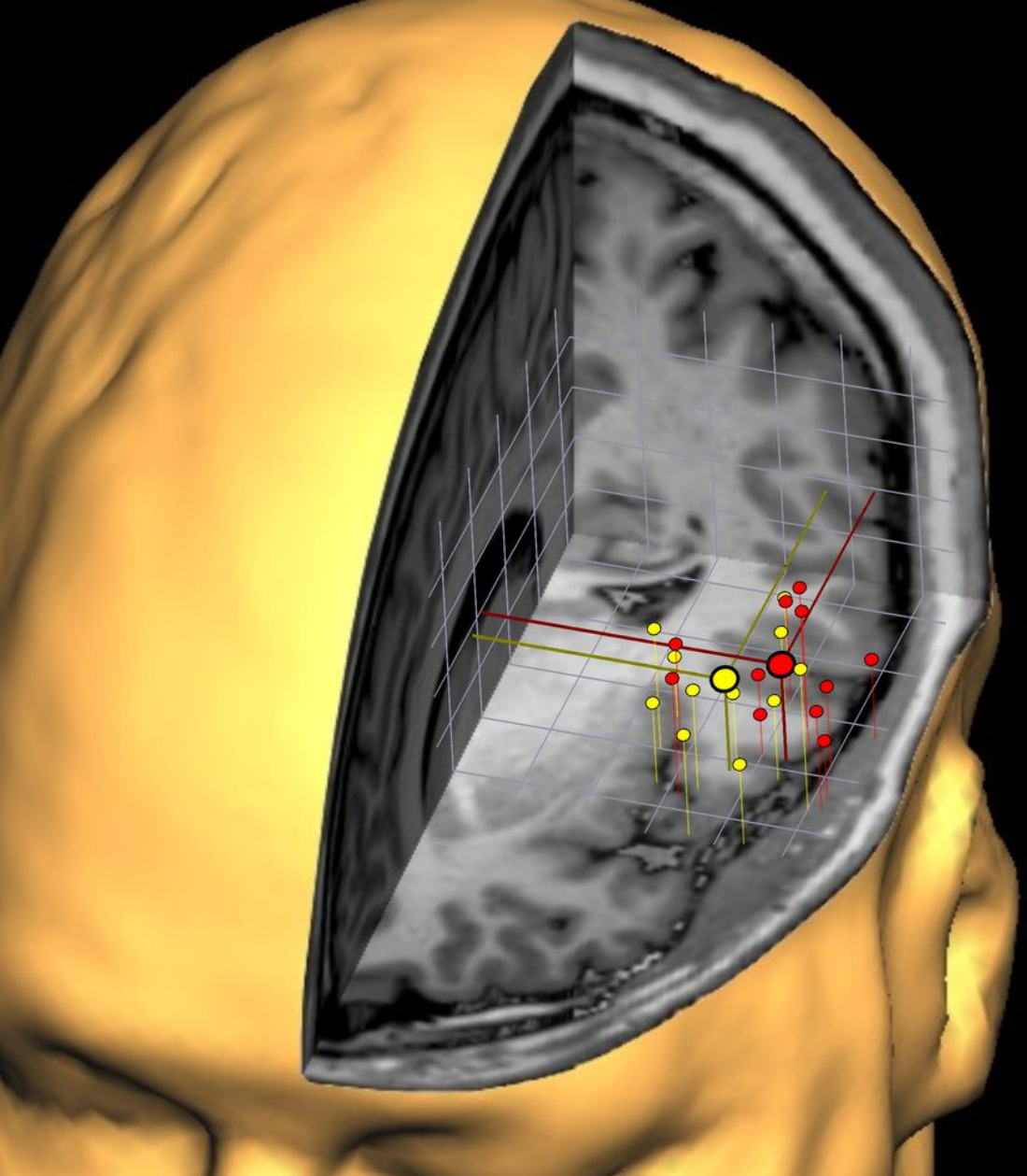

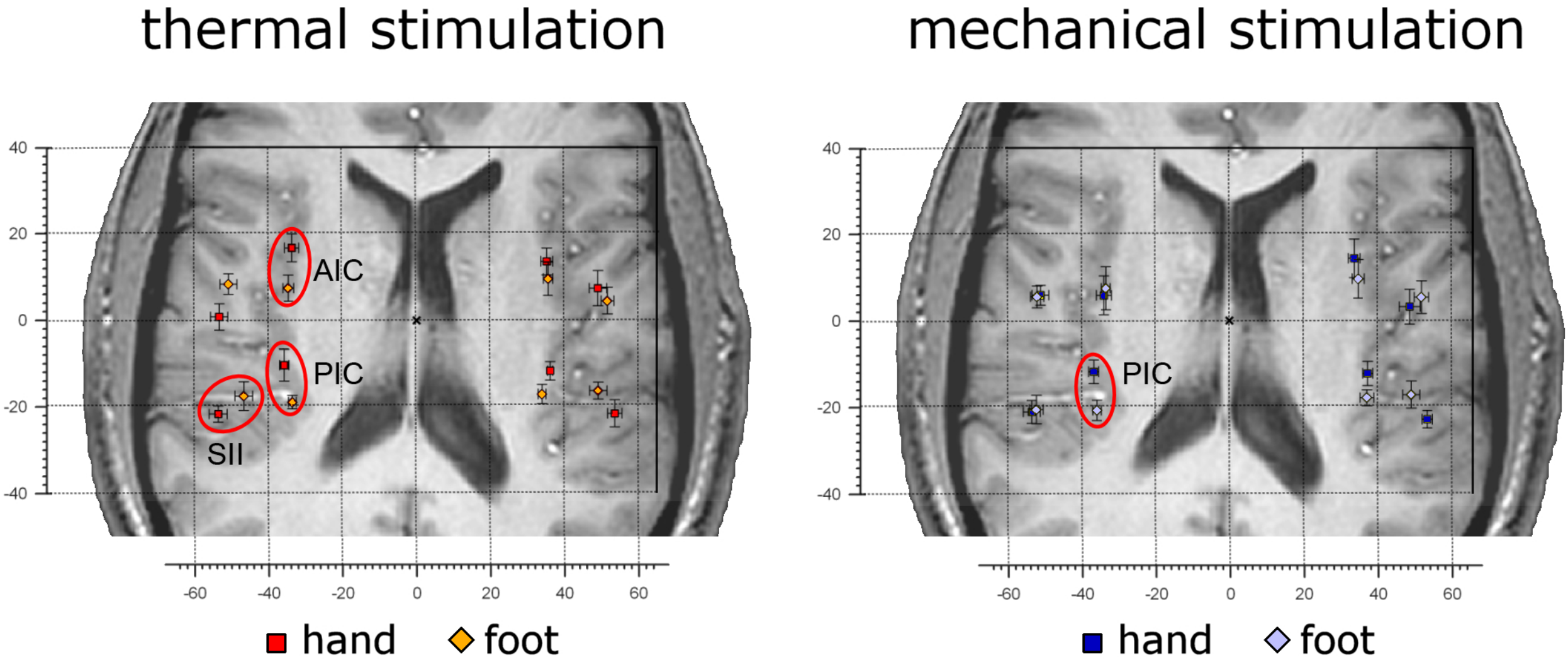
thermal stimulation
mechanical stimulation
AIC
PIC
SII
PIC
40
20
0
-20
-40
-60
-40
-20
0
20
40
60
hand
foot
hand
foot

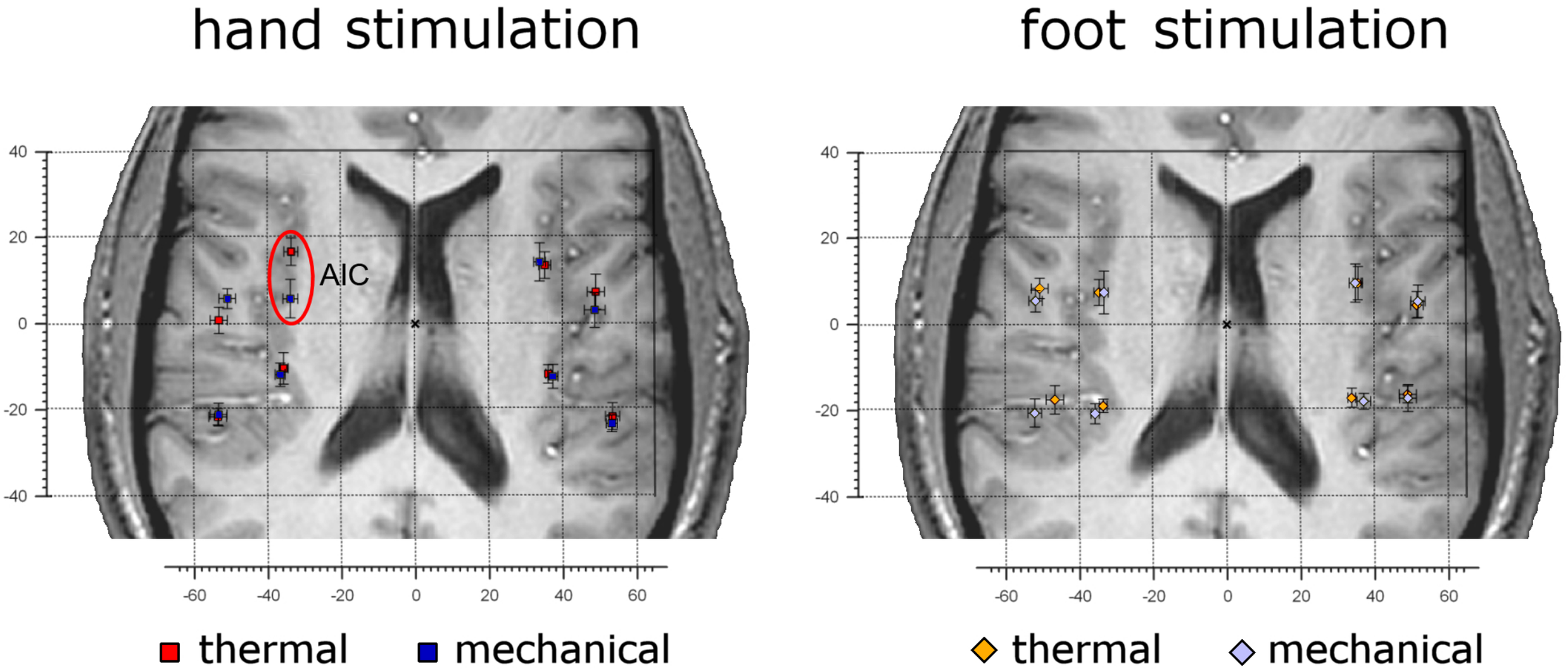
hand stimulation
foot stimulation
AIC
40
20
0
-20
-40
-60
-40
-20
0
20
40
60
thermal
mechanical
thermal
mechanical